Iranian Polymer Journal (2023) 32:1135–1148
https://doi.org/10.1007/s13726-023-01187-4

ORIGINAL RESEARCH

Effects of tomato peel extract on morphological, chemical, thermal, and mechanical properties of poly(lactic acid)

Erinc Kocak[1] · Mukaddes Sevval Cetin[2,3] · Ozlem Kizilirmak Esmer[1] · Hatice Aylin Karahan Toprakci[2,3]

Received: 24 January 2023 / Accepted: 9 May 2023 / Published online: 9 June 2023

Abstract

Poly(lactic acid) (PLA) is a sustainable, biodegradable polymer with high brittleness, elastic modulus, poor ductility, and low tensile strain that might restrict the packaging applications. The properties of PLA can be modified by addition of various materials. This study intended to reveal the effect of PLA with various concentrations of tomato peel extract (TPE) on the morphological, structural, thermal, and mechanical properties of PLA/TPE biocomposites. TPE was incorporated into the PLA matrix at 2, 4, and 6% w/w. The morphological analysis showed that films were successfully prepared by a combination of solvent-casting and compression-molding. TPE was well dispersed at low concentrations, though at higher concentrations above 2% w/w, an agglomeration of the TPE was observed. Thermal analysis revealed that the glass transition temperature of the biocomposites decreased with increasing content of TPE. FTIR spectra of the biocomposites showed that several components of TPE, such as phenolic compounds and fatty acid esters, could be incorporated into the matrix. Better mechanical performance was obtained for 2 and 4% w/w of TPE content in terms of tensile strain (between 2.4 and 38% higher compared to neat PLA) that was an indication of higher mechanical flexibility. These results showed the application performance of TPE in packaging materials.

Graphical abstract

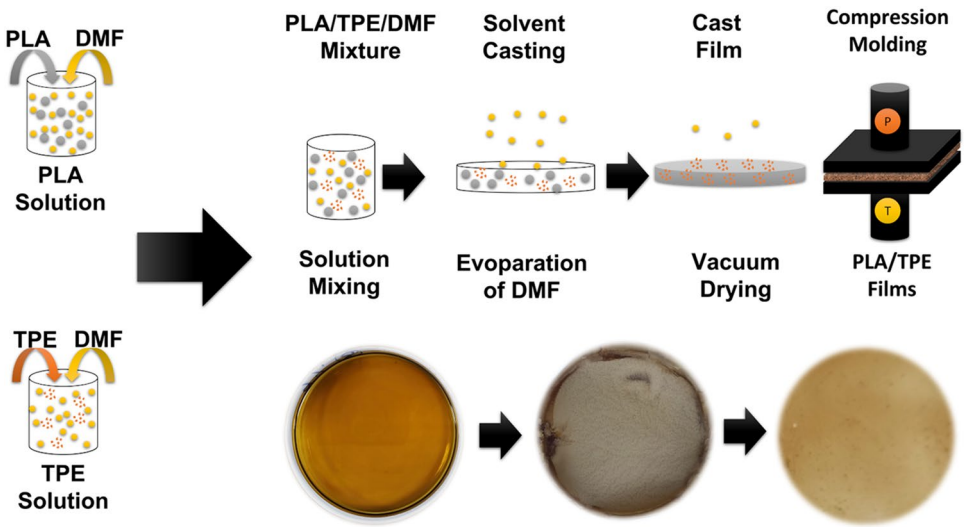

Keywords Poly(lactic acid) (PLA) · Tomato peel extract · Industrial food wastes · Bio-based composite · Biodegradable

Extended author information available on the last page of the article

Introduction

In the last few decades, the depletion of natural sources and global environmental pollution have been a great challenge that mankind has come to face. Particularly, in the packaging industry, several attempts have been made to generate eco-friendly products underlining biodegradability and sustainability concepts. In this regard, the use of biodegradable materials obtained from renewable, sustainable resources has drawn considerable attention. Poly(lactic acid) (PLA) is one of the biodegradable materials derived from sustainable natural sources [1]. It is biocompatible, processable, renewable, and energy-saving [2], highly transparent with good water barrier properties [3, 4], eco-friendly, and sustainable due to less CO_2 emission compared to hydrocarbon-based polymers [5, 6]. Despite these, it has several shortcomings such as high brittleness, poor ductility [7–9], low melt strength, low chemical and thermal stability [10–12], low elongation-at-break, and limited gas barrier properties [13–15]. High durability, pliability with little or no wrinkles (wrinkle-free), and easy processability are some fundamental considerations for packaging films [16–18]. Furthermore, flexibility is a significant property that should be evaluated by considering tensile stress and strain-at-break. To meet the desired mechanical properties for an ideal packaging material, PLA can be mixed with various natural ingredients including extracts [19, 20], essential oils [21–23], and their combinations [24, 25]. Green tea [19, 26], propolis [20, 23, 24], and carotenoid extracts [25] were some of the extracts used for obtaining PLA biocomposites. While green tea extract has been reported to decrease tensile strength, the strain-at-break is reported to increase [19]. On the other hand, the addition of Propolis extract led to increase in tensile strain and strength with a decrease in the elastic modulus [20]. Essential oils were the most common natural ingredients used in the literature. Anise oil/PLA composites showed a decline in tensile strength and an increase in strain-at-break [22]. Parallel with these outcomes; thyme, rosemary, and oregano-containing composite films, showed a decrease in tensile strength and a slight increase in strain-at-break [26]. It was also reported that the amount of oregano oil was significant in terms of strain-at-break and flexibility [21]. Essential oil/extract combinations were also reported in the literature to observe the synergistic effects. *Tanacetum balsamita* essential oil/Propolis extract containing PLA composites showed a drastic decrease in tensile strength and an increase in tensile strain when they were used together [23]. Similar results were also reported for *Thymus vulgaris*/Propolis containing PLA composites [24]. As mentioned above, the rigidity of the PLA limits its applications, and extracts, essential oils, or their combinations can increase flexibility. For this reason, in this research, it was aimed to enhance the mechanical properties in terms of strength and/or flexibility of PLA using tomato peel extracts.

Tomato is one of the most consumed agricultural products in the world regardless of the culture and region. Tomato is not only consumed in its fresh/dried fruit form but also in processed form. Sauces, juices, pastes, and peeled tomatoes are the processed form of tomatoes. To fabricate these products, tomatoes are peeled. Tomato production is ~ 180 million tons annually and ~ 45–50 million tons are used for industrial tomato-based products. A huge amount of waste composed of skins, fibers, and seeds (5–30% w/w of processed tomatoes) is generated from industrial tomato processing [27, 28] that is around ~ 8–8.5 million tons annually. Tomato peels (TP) build up 45% of these tomato wastes and this corresponds to ~ 3.5–4 million tons annually. TP includes several components, such as cutin, lignin, cellulose, hemicellulose, and waxes [29]. Among these, cutin is the major component that makes up 45–80% of TP and tomato is one of the agro-products with the highest cutin ratio [29, 30].

Cutin is a biopolyester-based polymeric network cross-linked by ester bonds [31]. It exhibits viscoelastic material behavior and imparts plasticity to TP [32] due to its structure composed of mainly polyhydroxy long-chain (C16-C18) fatty acids [30, 33, 34]. It contains some epicuticular waxes and several flavonoids (naringenin, chalconaringenin, etc.), phenolic compounds (ferulic and *p*-coumaric acid) as well that act as polymer fillers for reducing free space and consequently increase the rigidity of polymer matrix [35–37]. Other components of tomato peel extract (TPE) consist of cell wall polysaccharides, such as lignin, cellulose, and pectin, which are responsible for the stiffness of plant cuticles because of their rigid chain backbone [32]. Because of these properties, it was hypothesized that when TPE is used as a component, it may tune the morphological, thermal, and mechanical properties of biomaterials. It was seen that only a few studies with respect to the use of TPE for obtaining the packaging films either by polycondensation [38] or solvent-casting [39] were reported in the literature. However, there is not any study investigating the effects of TPE on biodegradable packaging material such as PLA. In this regard, to verify the hypothesis of TPE, it was used to tune the properties of PLA films, and this research aimed to determine the effects of different concentrations of TPE on the morphological, chemical, thermal, and mechanical properties of PLA biocomposite films by a combination of solvent-casting and compression-molding.

Experimental

Materials

PLA (96% L-lactic acid) (Luminy LX175) was kindly supplied by Total Corbion (The Netherlands). Before processing, it was dried in a vacuum oven at 80 °C for 4 h to remove the residual moisture. Fresh tomato pomace was supplied by a local tomato paste factory. Sodium hydroxide (NaOH), hydrochloric acid (HCl), and dimethylformamide (DMF) were purchased from Merck-Millipore. All the chemicals were used as received.

Preparation of TP

The tomato pomace was initially exposed to a sedimentation process that basically includes the separation of the seeds from the skins in water-filled containers. After removing the tomato seeds, the skins and fibers were dehydrated in a cabinet dryer at 60 °C for 8 h under the air flow rate of 1 m/s. Next, the dried tomato peels were milled using a hammer mill with a fixed rotor speed of 10 rpm for 30 s (50 g/min as feeding rate) (Brook Crompton 2000 Series, UK) and sieved by a mesh pore diameter of 500 µ (Retsch, Germany). The dried peels were stored at − 20 °C in vapor-proof, airtight packages until the extraction process started.

Alkaline extraction of TP

The extraction was carried out using the procedure described in the literature [29, 40]. The tomato peels were treated with NaOH solution (3% w/v) with the solvent/solute ratio of 10:1. After the filtration, the residue was washed twice with excess distilled water, and the supernatant was combined with the filtrate. Subsequently, the supernatant was acidified with 3 M of HCl until the pH of the solution reached 4.3. The samples were then centrifuged at 4000 rpm for 15 min three times by dialyzing with alkaline water (pH 8.45) until the pH reached 6.5. Afterward, the precipitates were freeze-dried using a freeze dryer for 12 h (Christ, Alpha 1–2 LD plus, Sweden). The freeze-dried TPE in sticky solid form was ground in mortar and pestle, weighed immediately and stored at − 18 °C in vacuum packages until the analysis started (Fig. 1).

Approximate composition analysis of TPE

The approximate composition analysis of TPE was performed gravimetrically as described by [29, 41].

Wax fraction

Briefly, a certain amount of TPE (4 g) was treated using a hexane/methanol mixture (3:1 v/v) to remove waxes. The mixture was filtered, and the filtrate which contained waxes was evaporated until constant dryness, and it was weighed and identified as a wax fraction (WX).

Polyphenols and water-soluble pectin fraction

The dewaxed TPE (the residue after the first filtration) was treated with boiling water for 10 min to recover polyphenols and water-soluble pectin. The mixture was filtered again and the supernatant that contained polyphenols and pectin was dried until constant weight and then weighed as polyphenol and water-soluble pectin fraction (PP).

Acid-soluble pectin fraction

In the following stage, the residue of the second filtration was acidified with 1 M and 0.5 M HCl, respectively, for 30 min at 85 °C twice to separate acid-soluble pectin. The solution was filtered, and the supernatant was dried until constant weight, weighed, and identified as acid-soluble pectin fraction (ASP).

Cutin fraction

The residue after the third filtration was treated with 1 M NaOH for 30 min at 85 °C three times. The supernatant of this stage was acidified with 3 M HCl and freeze-dried to yield cutin (C) as described in "Alkali extraction of TP" section.

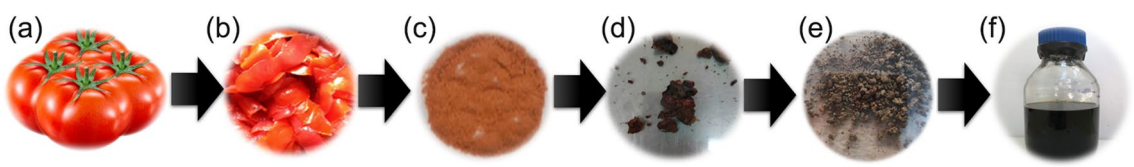

Fig. 1 Digital images of: **a** tomatoes, **b** fresh tomato peel, **c** dried powdered tomato peel, **d** freeze- dried TPE in sticky and clustered form, **e** freeze-dried TPE ground by mortar and pestle, and **f** TPE/DMF solution

Lignin and cellulose fraction

The residue of the final stage was treated with NaOCl (1.5%) at 95 °C twice for 1 h and then filtered to separate lignin from cellulose fraction, where the supernatant contained lignin fraction (L) and the residue contained cellulose (CF) after the final filtration.

Hemicellulose fraction

All the fractions including the supernatants in each stage and the final residues were dried until constant weight. The ratio of each component in the sample was calculated based on Eq. (1)

$$\text{Yield}\ (\%) = \left(w_f/w_i\right) \times 100, \tag{1}$$

where w_i presents the initial weight of the analyzed sample and w_f represents the final weight of the dried fraction.

The hemicellulose weight fraction (HC) was calculated using Eq. (2)

$$\text{HC}\ (\%) = \frac{\left[w_i - (\text{WX} + \text{PP} + \text{ASP} + \text{C} + \text{L} + \text{CF})\right]}{w_i} \times 100. \tag{2}$$

Preparation of the films

Polymeric films were prepared by a combination of solvent-casting and compression-molding (Fig. 2). Before mixing, two different solutions were prepared using DMF which was chosen, since both TPE and PLA are soluble in it. The PLA concentration was 10% w/w and the TPE concentration was 2% w/w. The films were around 3 g.

The cast films were dried at 80 °C for 24 h. After that to remove the solvent completely, samples were kept in a vacuum oven at 80 °C for 4 h. Since the thickness of the cast films was not very homogeneous after drying, films were compression molded between Teflon-coated plates at 200 °C for 15 s under 2.5 MPa. In the next step, samples were cooled down for 6 min until reaching room temperature under the same conditions. The sample codes of the films can be seen in Table 1.

Characterization

Morphological characterization

Field emission scanning electron microscope (FESEM) analysis was conducted with the instrument Thermo Scientific Apreo S that operated at 7.5 kV with a resolution between

Table 1 Sample codes and compositions

Sample code	TPE (% w/w)	PLA (% w/w)
PLA	0	100
TPE	100	0
PLA/TPE2	2	98
PLA/TPE4	4	96
PLA/TPE6	6	94

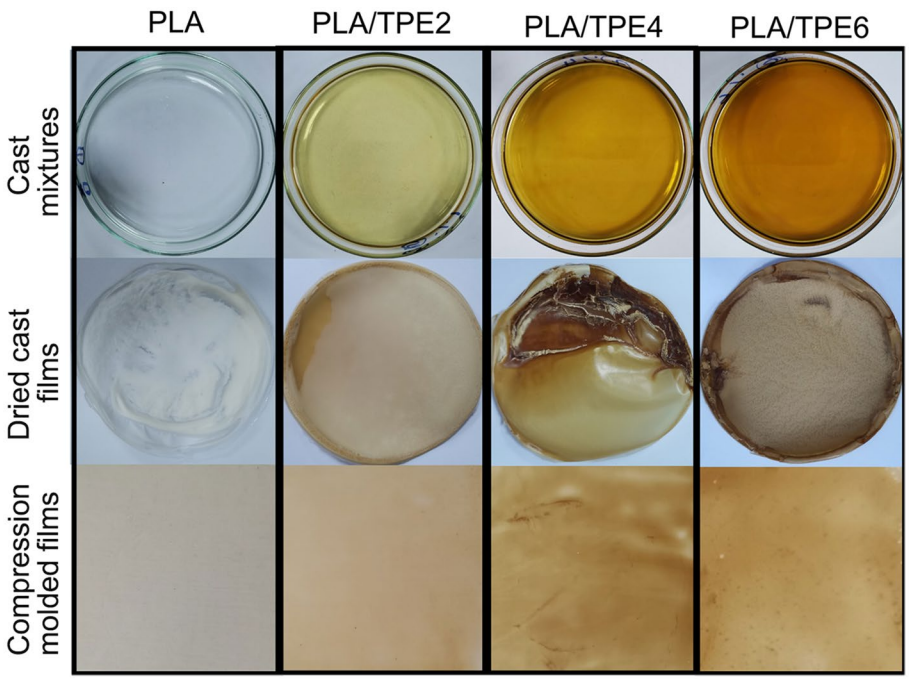

Fig. 2 Digital images of casted mixtures, dried casted films, and compression molded films

0.7 and 1.2 nm. The device was equipped with a Schottky electron source module. The samples were coated with gold (6–8 nm thickness) using a coating assembly (Leica EM ACE600). Both surface and edge images were captured. Digital image analysis was performed using Thermo Scientific AutoScript™ 4 Software–Python. The optical images were taken by a light microscope (AmScope 40X-2500X LED Digital Binocular Compound Microscope) and images were processed for obtaining high-contrast mode.

Fourier transform infrared spectroscopy (FTIR)

FTIR spectrums were provided using a Perkin Elmer Spectrum instrument with an ATR auto-sampling unit. While TPE was analyzed in powder form, the other samples were in film form. The spectra were collected over the range of 4000–650 cm^{-1}. For each sample, spectral scans were provided at a spectral resolution of 0.5 cm^{-1}. The data of the investigated samples were plotted as wavenumber versus transmittance (%).

Thermogravimetric analysis (TGA)

The TGA analysis was performed as the methodology described by Cifarelli et al. [40]. The mass loss (%) in TPE during progressive heat application between 20 and 600 °C was measured at a thermal increment of 5 °C/min using the TA instruments SDT–Q600 under a nitrogen atmosphere with a flow rate of 100 mL/min. A total of 10 mg of sample was inserted in an alumina crucible onto the sampling unit of the instrument. The change in mass was recorded, and a curve was obtained by plotting the percentage mass loss against temperature to indicate the degradation zone of the extracts. Weight loss (Δw) and derivative thermograms (DTG) were analyzed using TA instruments Universal analysis software.

Differential scanning calorimetry analysis (DSC)

The DSC analysis was based on the procedure described by Benitez et al. [29] with TA instruments Q20 model from − 50 to 200 °C under nitrogen flow at a flow rate of 50 mL/min. The accurately weighed samples (0.3 mg) were installed in the pans. Subsequently, a heating (1st)–cooling (1st)–heating (2nd) process was conducted. The first step involved heating from -50 °C to 200 °C, the second step involved cooling from 200 to − 50 °C, and the final step involved heating from − 50 to 200 °C by increments of 10 °C/min. The graph of temperature versus change in the heat flux was plotted for the second heating step. DSC thermograms were analyzed by Universal Analysis Software (TA instruments). The percentage crystallinity of PLA and biocomposites was calculated using Eq. (3)

$$X_c(\%) = \left[\left(\Delta H_m - \Delta H_c\right)/w\Delta H_{m0}\right] \times 100, \quad (3)$$

where ΔH_m and ΔH_c represent the experimental melt and cold crystallization enthalpies, respectively, and w is the weight fraction of PLA. ΔH_{m0} is the melt enthalpy for a theoretical fully crystalline PLA structure that was assumed to be 93 J g^{-1} as reported in the literature [42].

Mechanical analysis

The stress–strain behavior of the samples was determined by a universal mechanical testing system (Devotrans, DVT GPU/RD). The related graphs were given as engineering stress and strain. A digital thickness meter (Asimeto) was used for the determination of thickness. Specimens were cut from the film in both directions (x, y) with the dimensions of 5 × 15 mm (width × length), and for each sample, four specimens were used, average and standard deviation (SD) values were calculated. Samples were deformed under the test speed at 50 mm min^{-1}.

Results and discussion

The approximate composition of TPE

The analysis revealed that TPE obtained at 100 °C for 6 h contained several weight fractions including cutin (39.26% ± 0.70), hemicellulose (43.13% ± 0.58), acid-soluble pectin (4.25% ± 0.23), water-soluble pectin and polyphenols (2.84% ± 0.08), lignin (7.2% ± 1.54), and waxes (3.34% ± 0.41) based on the dry weight. To the best of our knowledge, there is no investigation in the literature that focuses on the composition of the TPE. The most abundant component in TPE has been found as hemicellulose. The reason for the high ratio of hemicellulose abundance in TPE might be that alkali treatment favored the extraction of several hemicelluloses such as xylan, the main hemicellulose in hardwood. It can be dissolved in an oligomeric form and easily gained by the alkali process [43].

Cutin was found as the second most abundant component. Its presence in tomato pomace was reported in earlier studies [29]. The ratio of lignin was determined in low amounts in TPE probably because the majority of lignin was removed during the washing step of the precipitate obtained after acidification in the extraction process. Mussatto et al. [44] reported that 68.5% of the lignin could be precipitated in the black liquor at a pH of 4.3, while 15.7% of lignin was precipitated at a pH of 6. Since the solution after washing and centrifuging had a pH of 6.5, most of the lignin was removed during the washing step [44].

While the low ratio of acid and water-soluble pectin was found in TPE, no cellulose could be determined in it, since

no residue was left after the treatment with NaOCl solution which means that all the solids left after alkali treatment were dissolved in NaOCl solution yielding only lignin fraction. Because the filtration process (with a mesh size of 300 µm) was performed on the supernatant after alkali extraction which removed the whole cellulose and some of the pectin moieties. To observe the effect of the filtration process on the ratios of the components, the same filtration was performed with a mesh size of 500 µ. In the TPE, filtered by a mesh size of 500 µm, cellulose, acid-soluble and water-soluble pectin ratios were found as 11.16 ± 2.26%; 10.97 ± 0.23%; 2.32 ± 0.38%, while cutin and hemicellulose ratios were calculated as 32.79 ± 2.43% and 28.87 ± 6.53%, respectively. These results revealed that filtration followed by alkali extraction significantly affected the composition of TPE.

Morphological characterization

The digital images of PLA/TPE mixtures, cast films, and compression molded films can be seen in Fig. 2. As it is obvious from the images, homogeneous films were fabricated of all compositions after compression-molding. The dark brown color of TPE/DMF solution can be seen in Fig. 1e. By increasing the TPE % w/w, the color of the sample became dark brownish. The light microscope images can be seen from the inset of mechanical test results. As seen at higher concentrations, TPE tends to agglomerate. Surface and edge SEM images of PLA film, TPE, and PLA/TPE biocomposite films are depicted in Fig. 3. As seen in Fig. 3a, neat PLA was successfully molten under given processing conditions, and a homogeneous, uniform film with a prominent smooth surface was obtained. On the other hand, the TPE had a more non-uniform structure with a rougher surface. As known, TPE exhibits a reticulate type of structural organization resulting from a branched network which predominantly consisted of 10, 16 dihydroxy hexadecanoic acid [45] and polyhydroxy acid was reported as the main component of tomato cutin [29, 40, 46]. Cutin is a polyester showing viscoelastic material behavior thanks to its sticky structure [32]. As given in Fig. 1c, the freeze-dried TPE was in sticky form. It is thought that cutin plays an important role in this sticky structure, since it consists of long-chain 16 or 18-carbon polyhydroxy fatty acids linked by cross-ester bonds, and cuticular waxes [29]. It was reported in the literature that cutin is responsible for the viscoelastic property of plant cuticles [47, 48] and sticky mass is obtained by an alkaline extraction of tomato peels [40].

Before SEM analysis, the sample was removed from the container by scraping it with a metal knife. Because of scraping out a sticky structure, small hill-like protuberances on the surface of TPE were observed with some irregularities. The ellipsoidal cells which are evident for the presence of tomato peel epidermis [39, 49] are visible on the SEM image of TPE (Fig. 3b). Surface and edge images of PLA/TPE biocomposite films can be seen in Fig. 3d–i. As it is obvious from the images, homogeneous film formation was obtained for all TPE concentrations. However, the PLA/TPE biocomposites indicated rougher surfaces with substantial non-uniformity that were assumed to be caused by

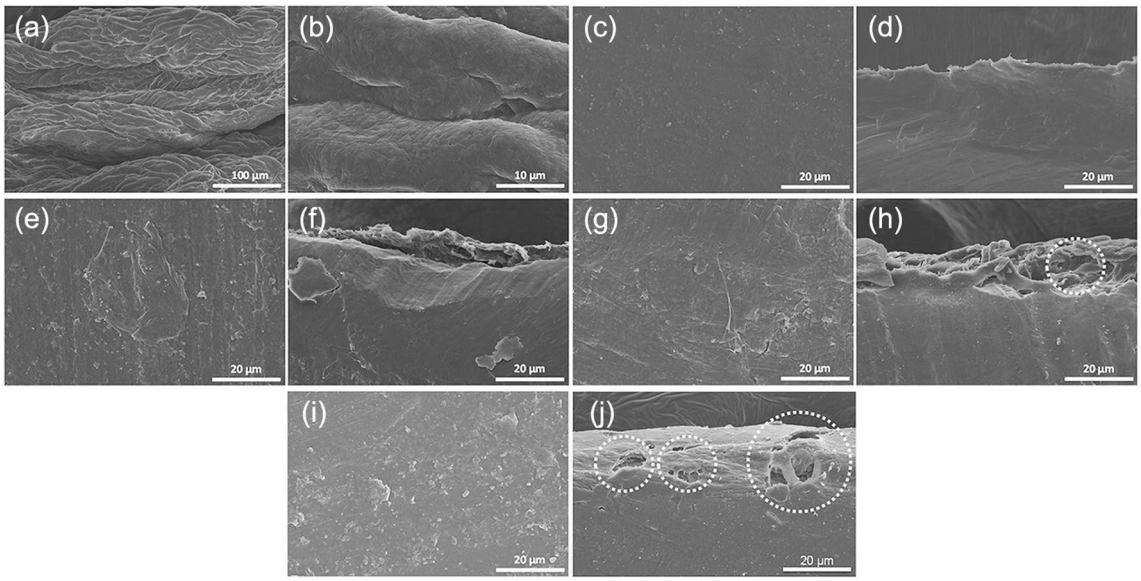

Fig. 3 SEM images of: **a** TPE surface (1kx); **b** TPE surface (10kx); **c** PLA film surface; **d** PLA film edge; **e** PLA/TPE2 film surface; **f** PLA/TPE2 film edge; **g** PLA/TPE4 film surface; **h** PLA/TPE4 film edge; **i** PLA/TPE6 film surface; and **j** PLA/TPE6 film edge (The magnifications of c, d, e, f, g, h, i, and j are 5kx)

an indented structure of neat TPE. Several researchers also confirmed the roughness of the surface in PLA composites reinforced with natural polymers [49]. Tedeschi et al. [50] reported that the roughness of sodium alginate films rose by the introduction of increasing content of tomato pomace monomers into sodium alginate. Several micro features, agglomerations, and low-volume cavities are visible on the edge images of PLA/TPE4 and PLA/TPE6 biocomposites (Fig. 3h and j) whereas PLA/TPE2 biocomposite appeared to have almost no features compared to the other biocomposites which were probably associated with increasing weight ratio of the TPE from 2 to 4 and 6% w/w. As the ratio of TPE increased in the composites, the number of polar hydroxyl groups present in cutin, hemicellulose and lignin also rose. Due to the increasing number of the polar hydroxyl groups, agglomeration occurred in TPE4 and TPE6. The polar hydroxyl groups had a high free surface energy and hence led to a greater attraction of molecules between each other which consequently gave rise to poor dispersibility and poor stability of the interfacial layer in these composites [51]. This can also be seen from optical light microscope images given in the inset of stress–strain graphs. At higher TPE concentrations, the density of black spots (TPE) increased noticeably. As a result, the composites became more prone to stress concentration and showed poorer mechanical properties. Similar outcomes were also reported for agro-extract filled PLA composites. As reported by [52, 53], increase in the extract amount led to rougher surface and formation of micropores throughout the composite thickness.

FTIR analysis

The results of the FTIR analysis are shown in Fig. 4a and b. The band assignments, specific to the neat PLA, were in accordance with the findings reported in earlier studies. The bands assigned in our study were as the following, as shown in Fig. 4a: Asymmetric and symmetric C–H stretching of methyl groups between 3000 and 2800 cm^{-1} [54–56]; C = O stretching at 1745 cm^{-1} [57, 58]; CH_3 bending at 1452 cm^{-1} [57] C–H-bending vibration of CH_3 at 1382 cm^{-1} [55, 59] and C–O stretching at 1267 cm^{-1} [59] C–O–C stretching at 1180 cm^{-1} [55, 58], –OH bending at 1041 cm^{-1} [58],

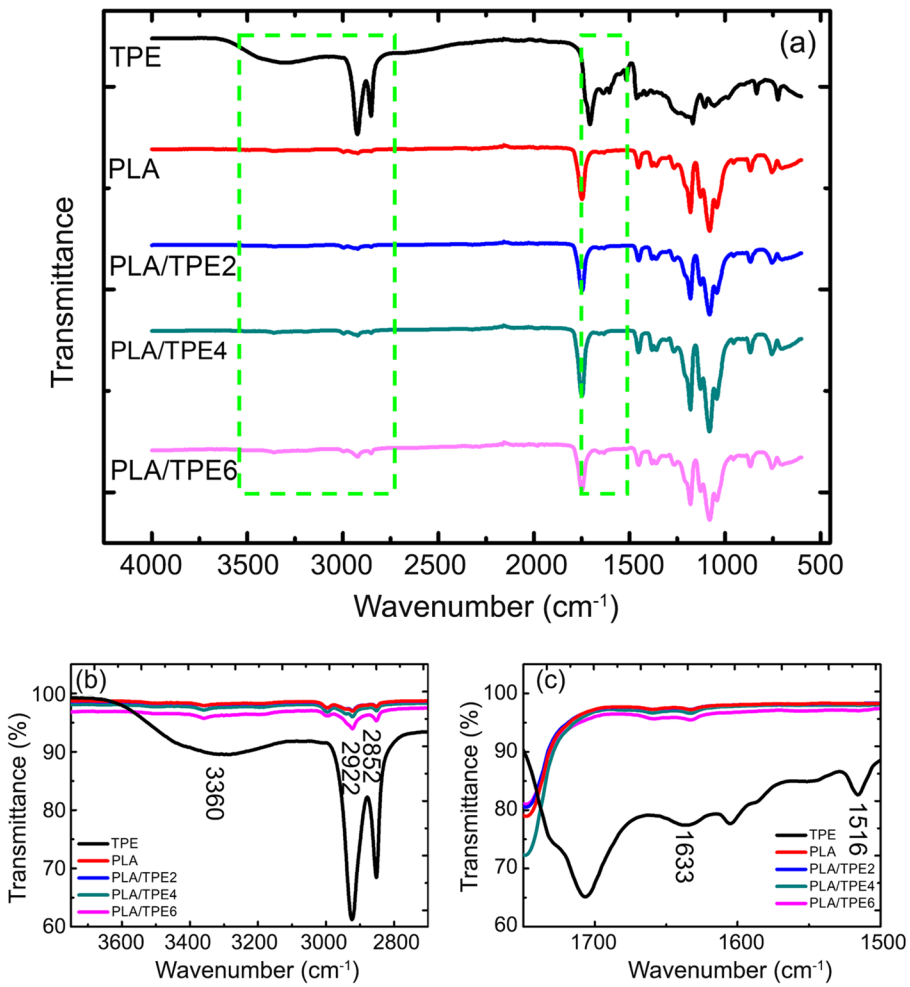

Fig. 4 **a** Stacked FTIR spectra of TPE, PLA, and PLA/TPE biocomposites between 4000 and 500 cm^{-1}, **b** between 3750 and 2750 cm^{-1}, and **c** 1750 and 1500 cm^{-1}

C–C stretching in amorphous phase at 865 cm^{-1} [58], C–C stretching in crystalline phase at 751 cm^{-1} [58], C = O out-of-plane bending at 696 cm^{-1} [60]. The FTIR spectrum of the neat TPE is presented in Fig. 4a. TPE exhibited several bands like PLA and several different bands from PLA. The band assigned in the range of 3600–3000 cm^{-1} was –OH stretching, and the bands at 2922 and 2852 cm^{-1} were associated with saturated aliphatic chains with asymmetric and symmetric CH_2 stretching, respectively [58–60]. The characteristic bands for TPE were assigned as the bands ascribed to C = O stretching of carboxylic acid at 1706 cm^{-1}; C = C stretching of phenolic acids at 1633 cm^{-1}; C–C stretching of phenolic compounds at 1607 and 1516 cm^{-1}; CH_2 bending at 1463 cm^{-1}; O–H bending at 1411 cm^{-1}; the carbonyl stretch of carboxylic acid to ester ν_a (C–O–C) band at 1167 and 1105 cm^{-1}; out-of-plane bending of C–H and C–C in phenolic compounds at 835 cm^{-1}; CH_2 bending at 723 cm^{-1}, respectively. In addition, several bands with respect to some cell wall polysaccharides were also detected in the FTIR spectrum of TPE. The band associated with xyloglucan, a common hemicellulose, was ascribed to C1–H β anomeric link bending at 897 cm^{-1}. The band with respect to pectin was assigned to C–O stretching at 1246 cm^{-1}. These band assignments are in agreement with the results reported by Szymanska-Chargot et al. [61], and Toscano et al. [62]. In addition, the FTIR spectrum of TPE is very similar to the spectrum of tomato peels reported by Mallampati et al. [63]. The characteristic absorptions for tomato peels after extraction were also assigned in the spectra of tomato peels as it was found in the study of these researchers.

Several bands associated with lignin (stretching of aromatic ring) and pectin (antisymmetric stretching of C = O carboxylate) might be overlapped with the C–C stretching of phenolic compounds; C = C stretching of phenolic acids at 1516 and 1633 cm^{-1}, respectively. The assignments for the overlapping bands with respect to lignin and pectin were reported by Toscano et al. [62]. It should be pointed out that the signals for the bands of all cell wall polysaccharides were much weaker compared to those assigned for cutin and phenolic compounds in the FTIR spectrum of TPE. This may be because the filtration of the DMF extract of tomato peels just before the introduction into PLA during solvent-casting provided the removal of a significant amount of cell wall polysaccharides from the TPE.

As shown in Fig. 4c, mainly the bands associated with phenolic compounds (1633, 1607, 1516, 835, and 723 cm^{-1}) in TPE were not detected in the spectrum of neat PLA. These findings were also parallel with the results of previous studies [29, 40, 46]. It was shown that the presence of several unsaturated, saturated fatty acids (oleic acid, linoleic acid, palmitic acid, and stearic acid), and phenolic compounds such as *p*-coumaric acid were presented in TPE [64]. In addition, based on our ongoing project results, it was determined that unsaturated, and saturated fatty acids, and several phenolic acids, such as *p*-coumaric acid, ferulic acid, 4-hydroxy benzoic acid, and caffeic acid, were found in TPE and that confirms the extraction process was successful [65].

The FTIR spectra between 3750 and 2750 cm^{-1} and 1750 and 1500 cm^{-1} are given in Fig. 4b and c, respectively. It was found that no significant changes occurred with respect to the chemical bonding of the neat PLA (Fig. 4b). This is an evidence of the occurring physical alterations (color, morphological structure) rather than chemical changes in the structure of the biocomposites compared to neat PLA films. However, it was found that the absorbance of several bands at 1411, 1516, 1633, 2852, 2922, and 3360 cm^{-1} associated with phenolic compounds and saturated aliphatic chains of TPE increased with the ascending weight ratios of TPE except for PLA/TPE2 which showed almost no change compared to the intensity of neat PLA. The intensities of these bands in all biocomposites indicated a high positive correlation ($R^2 = 0.725$; 0.768; 0.833; 0.805; 0.812; and 0.841; $p < 0.01$, respectively) with the weight ratios of TPE in the biocomposites. The band intensity increased linearly as the weight ratio of TPE increased from 2 to 6% in the biocomposites.

TGA analysis

Thermal degradation behavior of the samples between 20 and 600 °C is illustrated in TGA and DTG graphs in Fig. 5a and b, and the decomposition temperatures of the samples at $T_{d10\%}$, $T_{d50\%}$, and T_{dmax} are given in Table 2. TPE indicated three different major decomposition peaks at 198, 404, and 445 °C in the DTG graph. The peaks at 198 and 404 °C are the evidence for the presence of trihydroxy hexadecanoic acid and monohydroxy hexadecanoic acids, respectively [66]. The third peak that arose at 445 °C was reported as estolides which were formed because of the degradation of long-chain fatty acids and their oligomers [40]. However, these peaks were not observed in the DTG graphs of the biocomposites, since the weight ratios of TPE in the biocomposites were considerably low, and only a slight increase was observed for PLA/TPE6 as given inset image of Fig. 5b. The thermal degradation of PLA took place in one-step as previously reported [67]. PLA film started to degrade around 250 °C and showed T_{dmax} value at 341 °C. PLA/TPE biocomposites revealed a thermally stable behavior up to 220–250 °C with negligible weight losses that might occur due to the volatile compounds present in PLA and TPE [40]. However, when the thermal treatment proceeded to higher temperatures, all the biocomposites revealed a lower thermal stability compared to that of a neat PLA. The incorporation of TPE into PLA led to a drop in the thermal stability of the samples and $T_{d10\%}$, $T_{d50\%}$, and T_{dmax} decomposition temperature values declined. The T_{dmax} of the biocomposites

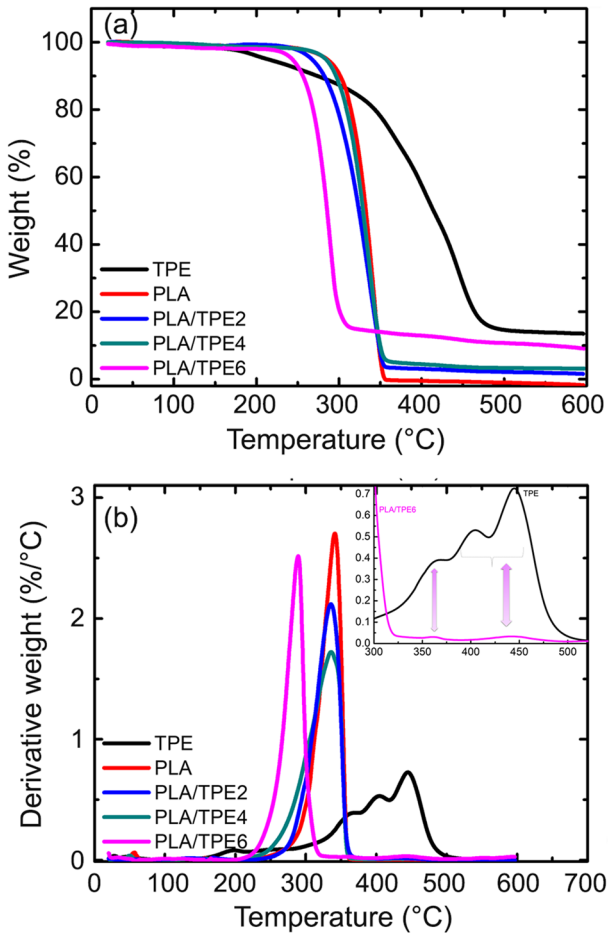

Fig. 5 **a** TGA and **b** DTG curves of PLA, TPE, and PLA/TPE biocomposites (inset: DTG curves of TPE and PLA/TPE6 between 300 and 550 °C)

Table 2 Thermal degradation behavior of PLA, TPE, and PLA/TPE biocomposites

Sample code	$T_{d10\%}$ (°C)	$T_{d50\%}$ (°C)	T_{dmax} (°C)	Weight loss at $T_{max\ degradation}$ (%)
PLA	301.50	332.55	341.26	72.19
TPE	273.84	414.50	445.00	68.10
PLA/TPE2	282.20	324.20	336.15	69.67
PLA/TPE4	296.37	329.19	336.03	64.29
PLA/TPE6	256.30	285.61	289.32	59.30

shifted slightly to lower values with the addition of 2% and 4% of TPE from 341 °C to 336 °C for both biocomposite films. When the content of TPE was further increased to 6%, T_{dmax} decreased drastically to 289 °C. That was assumed to be caused by the behavior of TPE between 200 and 250 °C. Although no significant difference was found between PLA/TPE2 and PLA/TPE4, PLA/TPE6 showed the lowest thermal stability because of higher TPE content. Similar results were also obtained in the study of Manrich et al. [39] to produce edible films by adding tomato peel-extracted cutin to pectin.

DSC analysis

The thermal behavior of PLA, TPE, and PLA/TPE biocomposites as a function of temperature is presented in Fig. 6. The thermal parameters, including glass transition temperature (T_g), cold crystallization temperature (T_c), crystallization enthalpy (ΔH_c), melting temperature (T_m), melting enthalpy (ΔH_m), crystallinity (X_c), and normalized crystallinity (X_{Sample}/X_{PLA}) values of the samples, were determined from the extracted data in Fig. 6 and given in Table 3. Since all samples showed flat plateau-type heat flow during cooling, no crystallization was observed, and no data were obtained in this step. Since 1st DSC run was carried out for creating similar thermal history to all samples, the discussion was given based on 2nd DSC run. T_c and T_m were obtained from the peak value of crystallization exotherm and melting endotherm, respectively. The degree of crystallinity was calculated from the following formula: $[(\Delta H_{m-}\Delta H_c)/\Delta H_{m0}]/w$ where ΔH_m, ΔH_c, $\Delta H_{m0,}$ and w are cold crystallization enthalpy of the sample, melting enthalpy of the sample, melting enthalpy for completely crystalline PLA, and weight fraction of PLA in the biocomposite, respectively. ΔH_{m0} of PLA was 93 J/g based on previous studies [42].

PLA is a semi-crystalline polymer and as it is obvious from Fig. 6; T_g, crystallization exotherm, melting endotherm peaks were observed and neat PLA exhibited a glass transition temperature (T_g) of 62.2 °C. The crystallization occurred during heating between 113 and 141 °C and the T_c was measured as 127.7 °C from the maximum value of crystallization exotherm peak. The melting occurred between

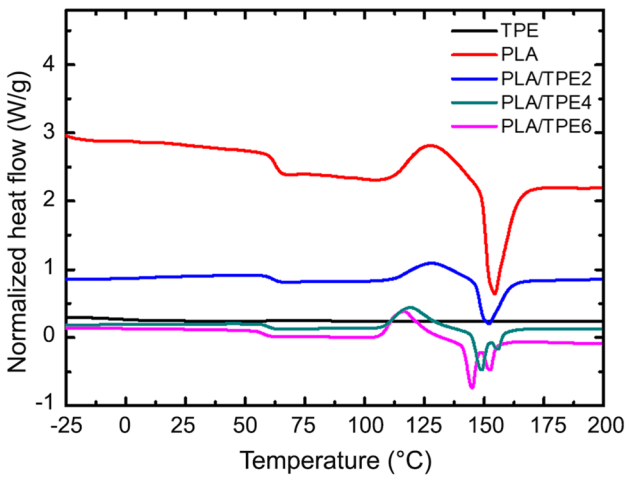

Fig. 6 The DSC thermograms of PLA, TPE, and PLA/TPE biocomposites

Table 3 Thermal parameters of PLA, TPE, and PLA/TPE biocomposites from DSC data (2nd run)

Sample code	T_g (°C)	T_c (°C)	ΔH_c (J/g)	T_m (°C)	ΔH_m (J/g)	X_c (%)	NX_c X_{Sample}/X_{PLA}
TPE	− 4.8	–	–	–	–	–	–
PLA	62.2	127.7	53.1	154.4	80.8	29.8	–
PLA/TPE2	61.0	127.6	21.0	151.9	30.3	10.2	0.34
PLA/TPE4	59.4	117.8	7.7	1* = 148.5	1* = 10.9	4.8*	0.16
				2* = 156.0	2* = 1.1		
PLA/TPE6	57.4	116.4	22.8	1* = 144.5	1* = 16.0	0.54*	0.02
				2* = 152.7	2* = 7.3		

*Since PLA/TPE4 and PLA/TPE6 biocomposites had two melting points, they were identified as 1 and 2 and the crystallinity of these biocomposites was calculated based on a total enthalpy change ($\Delta H_{total} = \Delta H_{M1} + \Delta H_{M2}$)

149 and 159 °C and a single T_m was measured as 154.4 °C from the peak of melting endotherm which is parallel with the previously reported outcomes [68–70]. X_c value for PLA was calculated as 29.8%. The T_g of TPE was determined at − 4.8 °C and neither crystallization exotherm nor melting endotherm was observed. PLA/TPE biocomposites also showed a similar trend in terms of heat flow with some differences compared to neat PLA. For all biocomposites, T_g, crystallization exotherm, and melting endotherm peaks were observed. The glass transition of PLA decreased with the increasing content of TPE in the biocomposites. T_g values of PLA/TPE2, PLA/TPE4, and PLA/TPE6 were determined as 61.0, 59.4, and 57.4 °C, respectively. As it is obvious from these results the higher the concentration of TPE in the biocomposite, the lower the glass transition temperature of the biocomposites. That was assumed to be caused by an increase in the segmental motion of PLA macromolecules because of TPE. As previously given, TPE showed relatively lower T_g compared to PLA and biocomposites showed T_g between PLA and TPE. Similar findings were also reported by Heredia-Guerrero et al. [71]. T_c/the interval of crystallization during heating was determined as 127.6/113–140, 117.8/110–126, and 116.4/108–124 °C for PLA/TPE2, PLA/TPE4, and PLA/TPE6, respectively. T_m/interval of melting during heating was determined as 151.9/146–158 °C for PLA/TPE2. For PLA/TPE4, two melting temperatures were observed as T_1 and T_2 at 148.5 and 156 °C, respectively, between 145 and 160 °C. Similar behavior was also observed for PLA/TPE6, and T_1 and T_2 were determined at 144.5 and 152.7 °C in the range between 141 and 155 °C, respectively. As can be seen, T_c and T_m of PLA/TPE2 have shifted to lower values compared to neat PLA. Unlike neat PLA and PLA/TPE2, two melting points (A/B and C/D °C) were observed for PLA/TPE4 and PLA/TPE6 biocomposites, respectively. As a result, the incorporation of TPE > 2% w/w into PLA caused an imperfect crystallinity in the biocomposites associated with the decrease in T_m. Likewise, the decline in T_g, a decrease in T_m and T_c was assumed to be caused by higher chain mobility and free volume [69]. X_c values of PLA, PLA/TPE2, PLA/TPE4, and PLA/TPE6 were calculated as 10.2; 4.8 and 0.54, respectively. As it is obvious from the results, the degree of crystallinity was found lower with higher TPE content.

Mechanical analysis

Stress–strain curves of PLA and PLA/TPE biocomposite films can be seen from Fig. 7a and b. Average tensile strength and tensile strain with SD values are summarized in Table 4 and Fig. 7b. PLA showed a typical stress–strain curve with 56.04 MPa tensile strength and 7.11% tensile strain. TPE concentration was found to be significant in terms of mechanical properties. Tensile strength/strain (%) values of PLA/TPE2, PLA/TPE4, and PLA/TPE6 were calculated as 57.15/9.85, 41.47/7.28, and 38.14/3.98, respectively. At 2% w/w TPE concentration, both tensile strain and tensile strength increased, and on the other hand, at 4 and 6% w/w, both properties dropped.

As known, PLA is a rigid polymer, and an increase in chain mobility and/or decrease in T_g can increase strain- and stress-at-break. In our case, 2% w/w TPE was found enough to increase the flexibility and resistance-to-break. However, at 4 and 6% w/w, TPE probably lowered the interaction between PLA chains, and samples have become more sensitive to applied stress. These outcomes can also be supported by SEM images and inset high-contrast light microscope images of the samples. As obvious from the images (Figs. 3e–j, Fig. 7b inset), by increasing the TPE ratio, a higher number of microfeatures and agglomerations were observed for PLA/TPE4 and PLA/TPE6. These microfeatures and agglomerations led to the formation of cavities as shown in edge images (Figs. 3h and j). Because of microcavity and agglomeration, the force bearing capacity of the biocomposites decreased which resulted in lower tensile strength and strain.

In literature, there are many studies on incorporation of low levels of agro-industrial waste extracts into PLA which reveal similar results with respect to morphological,

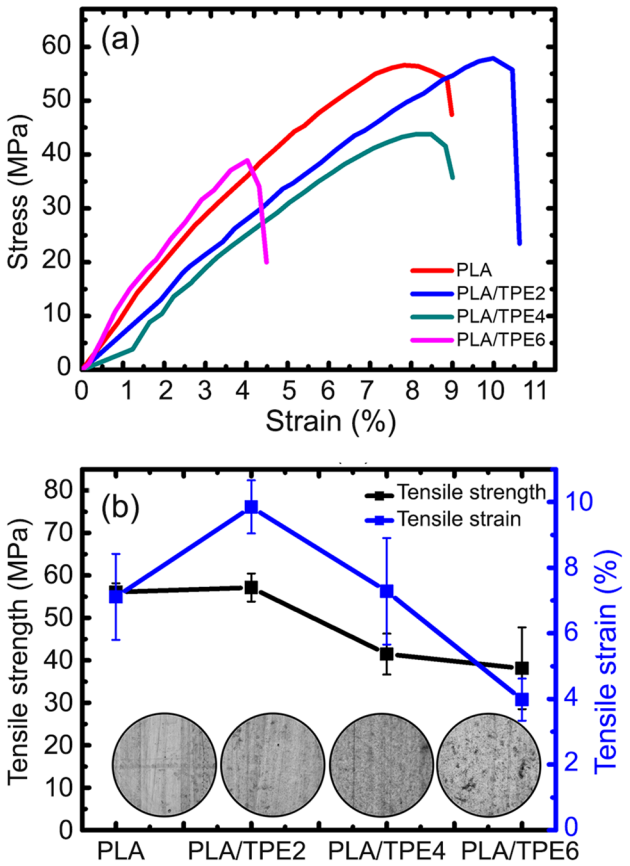

Fig. 7 **a** Stress–strain curves and **b** average tensile strength and strain values with optical images of PLA and PLA/TPE biocomposite films

Table 4 Mechanical properties of PLA, TPE, and PLA/TPE biocomposites

Sample code	Tensile strength (MPa)	SD	Tensile strain (%)	SD
PLA	56.04	2.07	7.11	1.31
PLA/TPE2	57.15	3.28	9.85	0.81
PLA/TPE4	41.47	4.82	7.28	1.62
PLA/TPE6	38.14	9.62	3.98	0.64

thermal, chemical, and mechanical properties of PLA. Since agro-extracts are low-molecular-weight materials, they can easily deteriorate the mechanical properties at very high concentrations. In a study, the addition of carrot pomace extract by 1% has led to an increase in tensile strength of PLA from 26.39 to 28.66 MPa, but further increase in the concentration to 4% led to lower tensile strength to 23.45 MPa [52]. In another study, addition of pomegranate peel extract (PEE) by 0.5–2% (by weight) together with zinc oxide nanoparticles at 3% (by weight) into PLA, the addition of 0.5% (by weight) PEE has led to a slight increase in tensile strength of neat PLA from 62.5 to 65 MPa. Higher concentrations have led to the reduction of tensile strength to 52.5 MPa. When low concentration of PEE (0.5% by weight) was incorporated, the surface morphology and cross-section changes of the composite films were thin and small, and the PEE particles on the surface of the composite were uniformly dispersed in the PLA/ZnO NPs matrix. With the increase of PEE content (1.5% by weight), the surface became rougher, and the micropores in the cross-section images became visible. In FTIR spectrum of all the composites, no significant new peaks were observed, indicating that PEE and ZnO NPs had a physical interaction only with the PLA rather than any chemical bonds, implying the successful preparation of the PLA-based composite film [53].

Conclusion

PLA biocomposites using different contents of TPE have been successfully prepared for the first time in the literature. SEM analysis revealed better morphological properties at 2% w/w of TPE content compared to other concentrations. FTIR analysis exhibited that the chemical properties of neat PLA remained unchanged by the incorporation of TPE. The presence of phenolic compounds and fatty acid esters in the biocomposites was verified by the results of FTIR analysis. The thermal stability of the films decreased with the increasing content of TPE. Nevertheless, films were thermally stable under processing conditions. TPE led to a decrease in T_g and crystallization temperature for biocomposites. Mechanical characterization revealed that optimum improvement in mechanical properties was obtained at 2% w/w of TPE content. The ultimate objective of this study was achieved by the improvement of flexibility and strength of biocomposites. This work is of significance not only for being the first attempt to prepare PLA/TPE composites but also for providing a quick route for the fabrication of sustainable biocomposites and investigating their properties. The future work will focus on the design and industrial fabrication of sustainable food packages from PLA/TPE films and the evaluation of their antioxidant, antimicrobial performance, and biodegradability in addition to morphological, mechanical, and structural properties.

Acknowledgements The present study was supported by the Ege University Scientific Research Projects Coordination with the Project ID: FGA-2022-23383.

Data availability The data supporting the findings of this study are available within the manuscript.

References

1. Xiao H, Yang L, Ren X, Jiang T, Yeh JT (2010) Kinetics and crystal structure of poly(lactic acid) crystallized nonisothermally: effect of plasticizer and nucleating agent. Polym Compos 31:2057–2068
2. Rasal RM, Janorkar AV, Hirt DE (2010) Poly(lactic acid) modifications. Prog Polym Sci 35:338–356
3. Gan I, Chow WS (2018) Antimicrobial poly(lactic acid)/cellulose bionanocomposite for food packaging application: a review. Food Packag Shelf Life 17:150–161
4. Edward MSG, Louis ACF, Srinivasan H, Venkatachalam S (2022) A mechanochemical approach for synthesizing almond shell nanoparticles and their potential application on the enhancement of polylactic acid film properties. Iran Polym J 31:1523–1535
5. Jamshidian M, Tehrany EA, Imran M, Jacquot M, Desobry S (2010) Poly-lactic acid: production, applications, nanocomposites, and release studies. Compr Rev Food Sci Food Saf 9:552–571
6. Muller J, González-Martínez C, Chiralt A (2017) Combination of poly(lactic) acid and starch for biodegradable food packaging. Materials 10:952
7. Sangeetha VH, Deka H, Varghese TO, Nayak SK (2018) State of the art and future prospectives of poly(lactic acid) based blends and composites. Polym Compos 39:81–101
8. Darie-Niţə RN, Vasile C, Irimia A, Lipşa R, Râpə M (2016) Evaluation of some eco-friendly plasticizers for PLA films processing. J Appl Polym Sci 133:43223
9. Ordoñez R, Atarés L, Chiralt A (2022) Properties of PLA films with cinnamic acid: effect of the processing method. Food Bioprod Proc 133:25–33
10. Barczewski M, Mysiukiewicz O, Szulc J, Kloziński A (2019) Poly(lactic acid) green composites filled with linseed cake as an agricultural waste filler. Influence of oil content within the filler on the rheological behavior. J Appl Polym Sci 136:47651
11. Dorgan JR, Lehermeier H, Mang M (2000) Thermal and rheological properties of commercial grade poly(lactic acids)s. J Polym Environ 8:1–9
12. Nofar M, Maani A, Sojoudi H, Heuzey MC, Carreau PJ (2015) Interfacial and rheological properties of PLA/PBAT and PLA/PBSA blends and their morphological stability under shear flow. J Rheol 59:317–333
13. Hemmati F, Farizeh T, Mohammadi-Roshandeh J (2021) Lignocellulosic fiber-reinforced PLA green composites: effects of chemical fiber treatment. In: Hameed Sultan MT, Majid MSA, Jamir MRM, Azmi AI, Saba N (eds) Biocomposite Materials. Composites Science and Technology. Springer, pp 97–204
14. Siakeng R, Jawaid M, Ariffin H, Sapuan SM (2019) Mechanical, dynamic, and thermomechanical properties of coir/pineapple leaf fiber reinforced polylactic acid hybrid biocomposites. Polym Compos 40:200–2011
15. Nofar M, Sacligil D, Carreau PJ, Kamal MR, Heuzey MC (2019) Poly(lactic acid) blends: processing, properties and applications. Int J Biolog Macromol 125:307–360
16. Van De Velde K, Kiekens P (2002) Biopolymers: overview of several properties and consequences on their applications. Polym Test 21:433–442
17. Pasha HY, Mohtasebi SS, Taherimehr M, Tabatabaeekoloor R, Firouz MS, Javadi A (2023) New poly(lactic acid)-based nanocomposite films for food packaging applications. Iran Polym J, In press
18. Biswas A, Cheng HN, Kuzniar G, He Z, Kim S, Furtado RF, Alves CR, Sharma BK (2023) Bilayer films of poly(lactic acid) and cottonseed protein for packaging applications. Polymers (Basel) 15:6
19. Martins C, Vilarinho F, Sanches Silva A, Andrade M, Machado AV, Castilho MC, Sá A, Cunha A, Vaz MF, Ramos F (2018) Active polylactic acid film incorporated with green tea extract: development, characterization and effectiveness. Ind Crops Prod 123:100–110
20. Safaei M, Roosta Azad R (2020) Preparation and characterization of poly-lactic acid based films containing propolis ethanolic extract to be used in dry meat sausage packaging. J Food Sci Technol 57:1242–1250
21. Llana-Ruiz-Cabello M, Pichardo S, Bermúdez JM, Baños A, Núñez C, Guillamón E, Aucejo S, Cameán AM (2016) Development of PLA films containing oregano essential oil (*Origanum vulgare* L. virens) intended for use in food packaging. Food Addit Contam Part A Chem Anal Control Expo Risk Assess 33:1374–1386
22. Noori N, Khanjari A, Rezaeigolestani M, Karabagias IK, Mokhtari S (2021) Development of antibacterial biocomposites based on poly(lactic acid) with spice essential oil (pimpinellaanisum) for food applications. Polymers (Basel) 13:3791
23. Khodayari M, Basti AA, Khanjari A, Misaghi A, Kamkar A, Shotorbani PM, Hamedi H (2019) Effect of poly(lactic acid) films incorporated with different concentrations of *Tanacetum balsamita* essential oil, propolis ethanolic extract and cellulose nanocrystals on shelf life extension of vacuum-packed cooked sausages. Food Packag Shelf Life 19:200–209
24. Ardjoum N, Chibani N, Shankar S, Ben FY, Djidjelli H, Lacroix M (2021) Development of antimicrobial films based on poly(lactic acid) incorporated with *Thymus vulgaris* essential oil and ethanolic extract of Mediterranean propolis. Int J Biol Macromol 185:535–542
25. Stoll L, Rech R, Flôres SH, Nachtigall SMB, de Oliveira RA (2019) Poly(acid lactic) films with carotenoids extracts: release study and effect on sunflower oil preservation. Food Chem 281:213–221
26. Zeid A, Karabagias IK, Nassif M, Kontominas MG (2019) Preparation and evaluation of antioxidant packaging films made of polylactic acid containing thyme, rosemary, and oregano essential oils. J Food Process Preserv 43:e14102
27. Szabo K, Cătoi AF, Vodnar DC (2018) Bioactive compounds extracted from tomato processing by-products as a source of valuable nutrients. Plant Food Human Nutr 73:268–277
28. Saini RK, Moon SH, Keum YS (2018) An updated review on use of tomato pomace and crustacean processing waste to recover commercially vital carotenoids. Food Res Int 108:516–529
29. Benítez JJ, Castillo PM, del Río JC, León-Camacho M, Domínguez E, Heredia A, Guzmán-Puyol S, Athanassiou A, Heredia-Guerrero JA (2018) Valorization of tomato processing by-products: fatty acid extraction and production of bio-based materials. Materials 11:2211
30. Ibrahim S, Riahi O, Said SM, Sabri MFM, Rozali S (2019) Biopolymers from crop plants. In: Reference module in materials science and Materials Engineering, Elsevier pp 1–10
31. Graça J (2015) Suberin: the biopolyester at the frontier of plants. Front Chem 3:62
32. López-Casado G, Matas AJ, Domínguez E, Cuartero J, Heredia A (2007) Biomechanics of isolated tomato (*Solanum lycopersicum* L.) fruit cuticles: the role of the cutin matrix and polysaccharides. J Exp Bot 58:3875–3883
33. Philippe G, Gaillard C, Petit J, Geneix N, Dalgalarrondo M, Bres C, Mauxion JP, Franke R, Rothan C, Schreiber L, Marion D, Bakan B (2016) Ester cross-link profiling of the cutin polymer of wild-type and cutin synthase tomato mutants highlights different mechanisms of polymerization. Plant Physiol 170:807–820
34. Parsons EP, Popopvsky S, Lohrey GT, Alkalai-Tuvia S, Perzelan Y, Bosland P, Bebeli PJ, ParanI FE, Jenks MA (2013) Fruit cuticle lipid composition and water loss in a diverse collection of pepper (Capsicum). Physiol Plant 149:160–174

35. Dominguez E, Heredia-Guerrero JA, Heredia A (2011) The biophysical design of plant cuticles: an overview. New Phytolog 189:938–949
36. Takahashi Y, Tsubaki S, Sakamoto M, Watanabe S, Azuma JI (2012) Growth-dependent chemical and mechanical properties of cuticular membranes from leaves of *Sonneratia alba*. Plant Cell Environ 35:1201–1210
37. Dominguez E, Espaa L, Lpez-Casado G, Cuartero J, Heredia A (2009) Biomechanics of isolated tomato (*Solanum lycopersicum*) fruit cuticles during ripening: the role of flavonoids. Funct Plant Biolog 36:613–620
38. Marc M, Risani R, Desnoes E, Falourd X, Pontoire B, Rodrigues R, Escórcio R, Batista AP, Valentin R, Gontard N, Pereira CS, Lopez C, Leroy E, Lourdin D, Marion D, Bakan B (2021) Bioinspired co-polyesters of hydroxy-fatty acids extracted from tomato peel agro-wastes and glycerol with tunable mechanical, thermal and barrier properties. Ind Crops Prod 170:113718
39. Manrich A, Moreira FKV, Otoni CG, Lorevice MV, Martins MA, Mattoso LHC (2017) Hydrophobic edible films made up of tomato cutin and pectin. Carbohydr Polym 164:83–91
40. Cifarelli A, Cigognini I, Bolzoni L, Montanari A (2016) Cutin isolated from tomato processing byproducts: extraction methods and characterization. In: 4th Int Conf Sustain 581 Solid Waste Manag 1–20
41. Szymanska-Chargot M, Chylinska M, Gdula K, Koziol A, Zdunek A (2017) Isolation and characterization of cellulose from different fruit and vegetable pomaces. Polymers (Basel) 9:495
42. Ferri JM, Garcia-Garcia D, Montanes N, Fenollar O, Balart R (2017) The effect of maleinized linseed oil as biobased plasticizer in poly(lactic acid)-based formulations. Polym Int 66:882–891
43. Schild G, Sixta H, Testova L (2010) Multifunctional alkaline pulping, delignification and hemicellulose extraction. Cell Chem Technol 44:35–45
44. Mussatto SI, Fernandes M, Roberto IC (2007) Lignin recovery from brewer's spent grain black liquor. Carbohydr Polym 70:218–223
45. Graça J, Lamosa P (2010) Linear and branched poly(ω-hydroxyacid) esters in plant cutins. J Agric Food Chem 58:9666–9674
46. Heredia-Guerrero JA, Benítez JJ, Domínguez E, Bayer IS, Cingolani R, Athanassiou A, Heredia A (2014) Infrared and raman spectroscopic features of plant cuticles: a review. Front Plant Sci 5:305
47. Scavée GML (2018) Synthesis and investigation of the bio-polymerization of cutin monomers and derivatives. PhD Thesis, Technical University of Denmark
48. Martin LBB, Rose JKC (2014) There's more than one way to skin a fruit: formation and functions of fruit cuticles. J Exp Bot 65:4639–4651
49. Bonilla J, Fortunati E, Vargas M, Chiralt A, Kenny JM (2013) Effects of chitosan on the physicochemical and antimicrobial properties of PLA films. J Food Eng 119:236–243
50. Tedeschi G, Benitez JJ, Ceseracciu L, Dastmalchi K, Itin B, Stark RE, Heredia A, Athanassiou A, Heredia-Guerrero JA (2018) Sustainable fabrication of plant cuticle-like packaging films from tomato pomace agro-waste, beeswax, and alginate. ACS Sustain Chem Eng 6:14955–14966
51. Chen K, Liao C, Li P, Li X, Li X, Zuo Y (2022) A compatible interface of wheat straw/polylactic acid composites collaborative constructed using KH570–nano TiO_2. J Polym Environ 30:2209–2221
52. Szymańska-Chargot M, Chylińska M, Pieczywek PM, Walkiewicz A, Pertile G, Frąc M, Cieślak KJ, Zdunek A (2020) Evaluation of nanocomposite made of polylactic acid and nanocellulose from carrot pomace modified with silver nanoparticles. Polymers (Basel) 12:812
53. Dai L, Li R, Liang Y, Liu Y, Zhang W, Shi S (2022) Development of pomegranate peel extract and nano ZnO co-reinforced polylactic acid film for active food packaging. Membranes (Basel) 12:1108
54. Cacciotti I, Mori S, Cherubini V, Nanni F (2018) Eco-sustainable systems based on poly(lactic acid), diatomite and coffee grounds extract for food packaging. Int J Biol Macromol 112:567–575
55. Brito GF, Agrawal P, Mélo TJA (2016) Mechanical and morphological properties of PLA/bioPE blend compatibilized with E-GMA and EMA-GMA copolymers. Macromol Symp 367:176–182
56. Wang Q, Hu Y, Zhu J, Liu Y, Yang X, Bian J (2012) Convenient synthetic method of starch/lactic acid graft copolymer catalyzed with sodium hydroxide. Bull Mater Sci 35:415–418
57. Jordá-Vilaplana A, Fombuena V, García-García D, Samper MD, Sánchez-Nácher L (2014) Surface modification of polylactic acid (PLA) by air atmospheric plasma treatment. Eur Polym J 58:22–33
58. Rocca-Smith JR, Karbowiak T, Marcuzzo E, Sensidoni A, Piasente F, Champion D, Heinz O, Vitry P, Bourillot E, Lesniewska E, Debeaufort F (2016) Impact of corona treatment on PLA film properties. Polym Degrad Stab 132:109–116
59. Zou H, Yi C, Wang L, Liu H, Xu W (2009) Thermal degradation of poly(lactic acid) measured by thermogravimetry coupled to Fourier transform infrared spectroscopy. J Therm Anal Calorim 97:929–935
60. Torres-Huerta AM, Del Angel-López D, Domínguez-Crespo MA, Palma-Ramírez D, Perales Castro ME, Flores-Vela A (2016) Morphological and mechanical properties dependence of PLA amount in PET matrix processed by single-screw extrusion. Polym Plast Technol Eng 55:672–683
61. Szymanska-Chargot M, Zdunek A (2013) Use of FT-IR spectra and PCA to the bulk characterization of cell wall residues of fruits and vegetables along a fraction process. Food Biophys 8:29–42
62. Toscano G, Pizzi A, Foppa Pedretti E, Rossini G, Ciceri G, Martignon G, Duca D (2015) Torrefaction of tomato industry residues. Fuel 143:89–97
63. Mallampati R, Valiyaveettil S (2012) Application of tomato peel as an efficient adsorbent for water purification—alternative biotechnology? RSC Adv 2:9914–9920
64. Midhun Prasad K, Murugavelh S (2020) Experimental investigation and kinetics of tomato peel pyrolysis: performance, combustion and emission characteristics of bio-oil blends in diesel engine. J Clean Prod 254:120115
65. Kızılırmak Esmer Ö, Koçak E, Cevrem AE, Kıcıkoğlu O (2022) Alkali extraction of phenolic compounds from tomato peel: optimization of extraction conditions and investigation of phenolic profile by LC-MS/MS. Turk J Agric Food Sci Technol 10:2966–2976
66. Benítez JJ, Heredia-Guerrero JA, Guzmán-Puyol S, Barthel MJ, Domínguez E, Heredia A (2015) Polyhydroxy ester films obtained by non-catalyzed melt-polycondensation of natural occurring fatty polyhydroxyacids. Front Mater 2:1–10
67. Mandal DK, Bhunia H, Bajpai PK (2019) Thermal degradation kinetics of PP/PLA nanocomposite blends. J Thermoplast Compos Mater 32:1714–1730
68. Hassouna F, Raquez JM, Addiego F, Dubois P, Toniazzo V, Ruch D (2011) New approach on the development of plasticized polylactide (PLA): grafting of poly(ethylene glycol) (PEG) via reactive extrusion. Eur Polym J 47:2134–2144
69. Rapa M, Nita RND, Vasile C (2017) Influence of plasticizers over some physico-chemical properties of PLA. Mater Plast 54:73–78
70. Cao X, Mohamed A, Gordon SH, Willett JL, Sessa DJ (2003) DSC study of biodegradable poly(lactic acid) and poly(hydroxy ester ether) blends. Thermochim Acta 406:115–127

71. Heredia-Guerrero JA, Goldoni L, Benítez JJ, Davis A, Ceseracciu L, Cingolani R, Bayer IS Heinze T, Koschella A, Heredia A, Athanassiou A (2017) Cellulose-polyhydroxylated fatty acid ester-based bioplastics with tuning properties: acylation via a mixed anhydride system. Carbohydr Polym 173:312–320

Authors and Affiliations

Erinc Kocak[1] · Mukaddes Sevval Cetin[2,3] · Ozlem Kizilirmak Esmer[1] · Hatice Aylin Karahan Toprakci[2,3]

✉ Hatice Aylin Karahan Toprakci
aylin.toprakci@yalova.edu.tr

[1] Food Engineering Department, Ege University, Bornova, 35100 Izmir, Turkey

[2] Department of Polymer Materials Engineering, Yalova University, 77200 Yalova, Turkey

[3] Institute of Graduate Studies, Yalova University, 77200 Yalova, Turkey